Lab on a Chip

Accepted Manuscript

ROYAL SOCIETY OF CHEMISTRY

www.rsc.org/loc

Journal Name

RSCPublishing

ARTICLE

Preparation and mechanical characterisation of giant unilamellar vesicles by a microfluidic method

Cite this: DOI: 10.1039/xoxxoooooox

K. Karamdad,[ab] R. V. Law [ab], J.M. Seddon [ab], N. B. Brooks[ab] and O. Ces*[ab]

[a] Department of Chemistry, Imperial College London, Exhibition Road, London, SW7 2AZ.
[b] Institute of Chemical Biology, Imperial College London, Exhibition Road, London, SW7 2AZ.

Received ooth January 2012,
Accepted ooth January 2012

DOI: 10.1039/xoxxoooooox

www.rsc.org/

Giant unilamellar vesicles (GUVs) have a wide range of applications in biology and synthetic biology. As a result, new approaches for constructing GUVs using microfluidic techniques are emerging but there are still significant shortcomings in the control of fundamental vesicle structural parameters such as size, lamellarity, membrane composition and internal contents. We have developed a novel microfluidic platform to generate compositionally-controlled GUVs. Water-in-oil (W/O) droplets formed in a lipid-containing oil flow are transferred across an oil-water interface, facilitating the self-assembly of a phospholipid bilayer. In addition, for the first time we have studied the mechanical properties of the resultant lipid bilayers of the microfluidic GUVs. Using fluctuation analysis we were able to calculate the values for bending rigidity of giant vesicles assembled on chip and demonstrate that these correlate strongly with those of traditional low throughput strategies such as electroformation.

Introduction

The lipid bilayer is a universal component of all cell membranes. It is ubiquitous across a vast range of cellular processes and a highly complex supramolecular structure. The significance of the lipid bilayer to various cellular processes has prompted a deluge of membrane models to be developed. Lipid bilayers that are assembled *in vitro* must replicate the key properties of biological membranes such as bilayer size, curvature and shape, lamellarity, asymmetry and the capacity to accommodate functional transmembrane proteins.

GUVs are cell-sized aqueous spheres enclosing an internal aqueous environment and bounded by a phospholipid bilayer. They can exhibit the full scope of the aforementioned traits related to plasma membranes. The advantage of using GUVs as a 'bottom-up' model system is that they can be worked into more elaborate models of biomolecular self-organization. They have been reported for use in a wide range of biological and chemical applications including protein screening, drug delivery and immunoassays[1–3].

Various bulk methods, such as extrusion, gentle hydration and electroformation, have been synonymous with the formation of lipid vesicles over recent years[4–6]. However the shortcomings associated with these processes, such as vesicle size disparity and lack of membrane asymmetry have paved the way for the development of improved formation methods.

Microfluidic techniques for producing vesicles have emerged in recent years because of the high reproducability and control introduced by new methods[7]. Droplet emulsion approaches challenge the more traditional bulk methods as they put the control over key parameters in the hands of the user[8].

One of the biggest limitations to date, with regards to lipid vesicle forming techniques, is the inability to selectively control the distribution of lipids across the midplane membrane bilayer. This is a troubling limitation as biological plasma membranes are highly asymmetric and it remains unclear as to how this characteristic may effect the mechanical properties of the membrane[9].

The highly complex mechanical behaviour of lipid membranes is a burgeoning area of investigation. This is because very minor changes in the mechanical properties are critical to a wide range of general and highly specific functions of the cell, for example, it has been suggested that deformations in the plasma membrane control the gating mechanism of mechanosensitive channel proteins[10]. The mechanical properties also impact the binding of specific proteins to the membrane bilayer. The torque tension and spontaneous elastic curvature of the bilayer have been both been found to effect the degree of protein binding in the membrane[11,12]. Understanding morphological changes in the membrane requires a more detailed knowledge of membrane elastic properties. Biological membranes possess certain mechanical properties, such as a very low bending rigidity, which allow for changes in the morphological state of the cell[13]. Previously the bending rigidity of lipid membranes assembled in GUVs constructed *via* low throughput strategies, such as electroformation, have been reported as a function of various conditions. The impact of temperature and the presence of various other inclusions in the bilayer, such as cholesterol, have been found

to have affected bending rigidity measurements[14,15]. The lipid composition of the bilayer is also critical in effecting membrane rigidity, κ with properties such as lipid chain length and degree of saturation having both been found to have an impact[16].

We have developed a microfluidic technique to form lipid vesicles in high throughput with full control over the composition of the membrane. This is achieved through the means of producing microfluidic channels with a step junction, produced by double-layer photolithography, which facilitates the transfer of a W/O emulsion across an oil-water phase boundary. We report the formation of symmetric GUVs assembled on chip using saturated phosphocholine lipid, DPhPC, and the unsaturated lipid, POPC (as described in **ESI-SI 1**). To confirm the presence of a functional lipid bilayer, we reconstituted the protein pore α-hemolysin into the membrane and studied the resultant time-dependent leakage of fluorescent molecules from the vesicles.

Previously the bending rigidity of lipid membranes has been measured using thermal fluctuation analysis[17–19]. Imaging vesicle contours at high speeed using phase contrast microscopy allows for the quantitative measurement of the amplitudes of equatorial modes of these fluctuations.

GUVs have been ubiquitous as a model for the biophysical study of membrane rigidity; here we validate for the first time the manufacture of GUVs using microfluidics by analyzing the thermal fluctuations of microfluidic GUVs assembled on chip to give a value for bending rigidity, κ for symmetric giant vesicles composed of DPhPC.

Results and Discussion

Giant vesicle generation

The initial W/O emulsions were generated *via* a flow focus mechanism (Figure 1a), where the internal aqueous encapsulant was sheared by a carrier oil phase flow. The resulting W/O emulsions were stabilised by lipids dissolved in squalene oil (DPhPC, 5mg/ml^{-1}), which spontaneously formed a monolayer around the aqueous droplets in the meander (Figure 1b). Control over the internal aqueous flow rate (Q_{IW}) and oil flow rate (Q_O) directly affected the regime of droplet formation; droplet diameter decreased with decreasing Q_{IW} and also decreased with increasing Q_O. The flow rate of the external aqueous phase (Q_{EW}) had no bearing on the dimensions of the initial W/O emulsions.

Upon arrival at the 'step' junction the plug-shaped W/O emulsions spontaneously transformed into spherical droplets (Figure 1c), this was due to the channel geometry becoming deeper. Once transferred into the deeper hydrophilic channel carrying the external aqueous phase the spherical W/O/W droplets were bounded by an outer monolayer of lipids from small vesicles (DPhPC, 3mg/ml^{-1}) in the aqueous phase.

The hydrophilic modification of the PDMS of the external aqueous channel was instrumental in releasing the emulsions from the oil

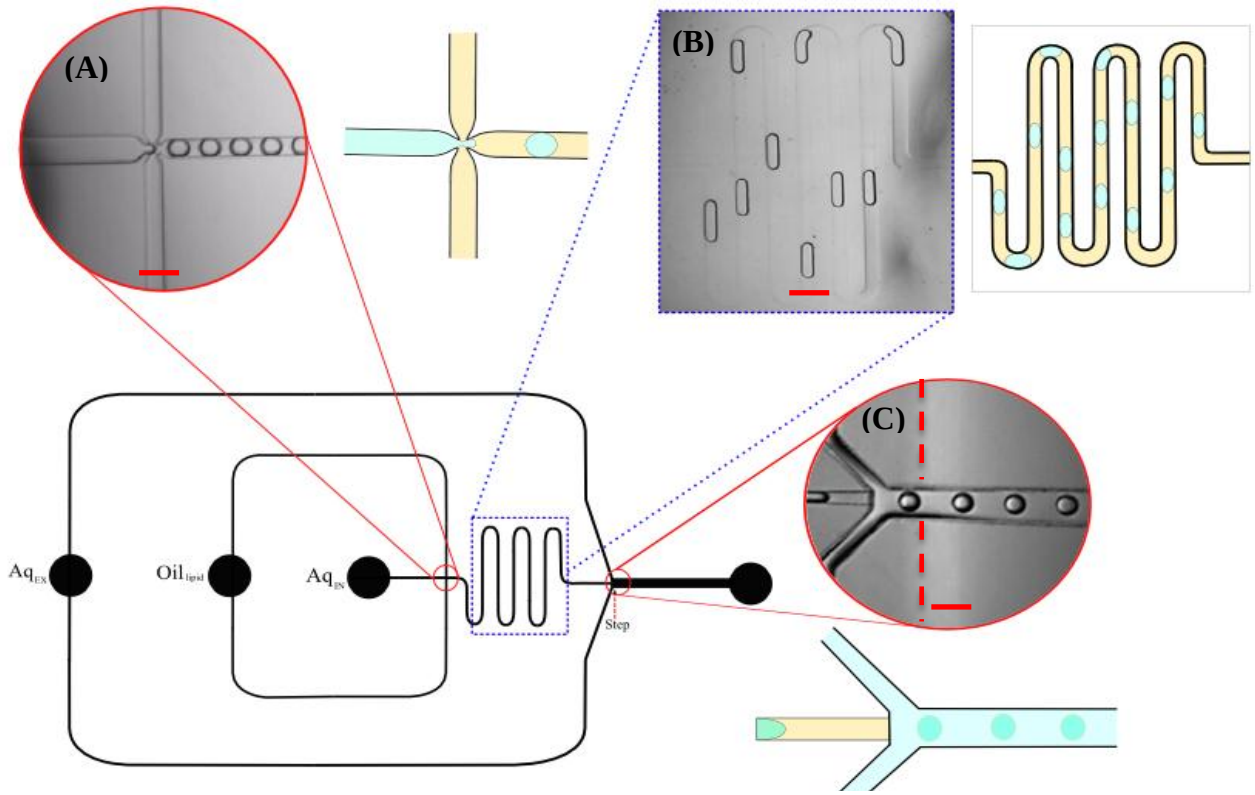

Figure 1: Schematic and images of vesicle production line. (A) Image of the flow focussing junction where the internal aqueous dispersed phase (Aq_{IN}) is sheared by a carrier oil flow to produce monodisperse W/O emulsion (scale=70μm). (B) Image of the channel meander, which allows for the spontaneous formation of a lipid monolayer around each aqueous droplet (scale=80μm). (C) Image of the step junction, whereby the channel carrying the initial W/O droplets changes in depth (from 50μm to 100μm) to allow the emulsions to transfer into the external aqueous phase (Aq_{EX}) (scale=100μm). The change in refractive index indicated on the image (dashed red line) illustrates where the PDMS has been treated in the deeper channel to prevent the wetting of each droplet on the channel wall.

phase into the aqueous phase. This hydrophilic modification for microfluidic applications was reported previously by Yao *et al*[20], where the contact angle with an aqueous droplet was found to change from 110˚ to as low as 21.5˚.

The size and structure of the droplets upon phase transfer were maintained in the external aqueous channel. The step junction proved to be a viable mechanism in which to transfer W/O droplets across the oil-water phase boundary without rupture or leakage of internal contents of the droplets.

By adjusting the flow rates, we were able to exert a fine control over the diameter of the W/O emulsions and thus the assembled GUVs. Vesicles in the range of 40 to 80µm were formed using this device. The distributions of the diameter of the microfluidic GUVs, formed at specific flow rates, were found to be very narrow with a polydispersity coefficient of 3.1% (Figure 2).

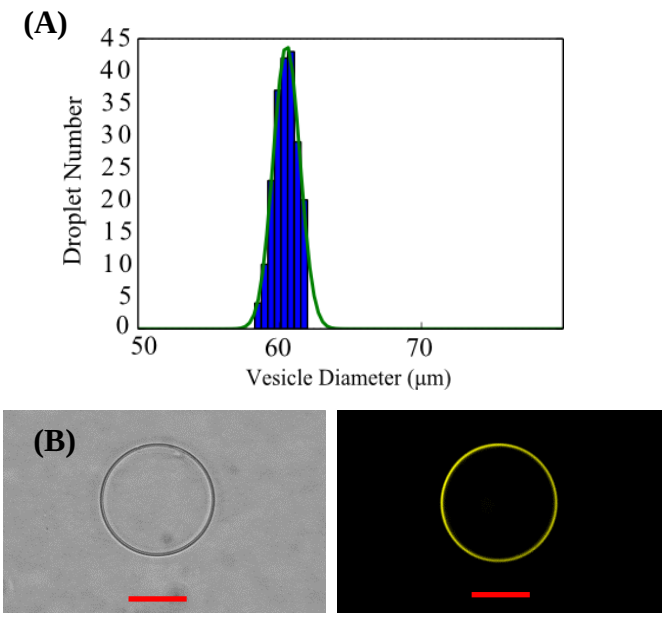

Figure 2: (A) Diameter distribution of the microfluidic GUVs assembled on chip. The average diameter for this data set (N=200) is 60.5µm with a polydispersity coefficient of 3.1%. These vesicles were produced at specific flow rates of Q_{IW} = 0.10µl min^{-1}, Q_O = 1.50µl min^{-1} and Q_{EW} = 50.00µl min^{-1} respectively. (B) Bright field and fluorescence microscopy images of a microfluidic vesicle (scale=20µm) labelled with 0.5 wt% fluorescent lipid, N-lissamine rhodamine B DPPE (Rh-PE), in the inner leaflet of the membrane.

A critical consideration in the formation of these giant vesicles is the interfacial tension of the oil-water phase boundary. Saeki *et al* previously reported the formation of W/O/W droplets using a multi-depth microfluidic system[21]. They confirmed that the use of surfactant caused a decrease in the interfacial tension of the oil-water phase boundary, which allowed for the release of the W/O droplets into the external aqueous phase to form robust W/O/W emulsions. Here a similar principle was applied using lipids to yield the same effect.

The external aqueous phase contained sonicated vesicles, which adsorbed at the oil-water interface of the initial emulsions to form a stable bilayer and thus a vesicle. Without the inclusion of extruded vesicles in the external aqueous phase vesicles did not form.

Emulsions, whether produced in bulk or on chip, have been widely used as vesicle precursors due to the ability to control the internal contents, size and membrane composition[22-25]. As well as demonstrating these elements of GUV control, our technique for generating vesicles is a continuous process. This is advantageous especially when compared to batch production techniques such as emulsion phase transfer[22]. Generating GUVs in such high throughput gives scope for much more efficient collection of large sets of data. However, a resonant concern of using emulsions as vesicle templates is the presence of residual oil in the bilayer[22–25]. This problem has been ubiquitous when forming GUVs from water-in-oil precursors and has been proposed to affect the biophysical and elastic properties of lipid membranes. Our technique, by no means, is exempt from this phenomenon however we aim to characterise whether residual oil in the bilayer has any effect on the membrane mechanical properties using fluctuation analysis.

Protein insertion experiments

In order to confirm the presence of a unilamellar bilayer we performed a series of fluorescence leakage assays in the microfluidic GUVs. This was done by successfully reconstituting the transmembrane protein, alpha-hemolysin (αHL), into the bilayer of the GUVs. αHL is a water-soluble protein monomer which assembles in unilamellar membranes to oligomerize into a heptameric, water-filled pore. In biology these pores lead to lysis and cell death[26]. In this context the protein was encapsulated into the internal aqueous environment of the initial droplets along with water-soluble fluorescent molecules. Upon the assembly of the membrane bilayers in these droplet systems, we observed the leakage of the fluorescent molecules (Fig. 3) due to the spontaneous process of αHL self-assembly.

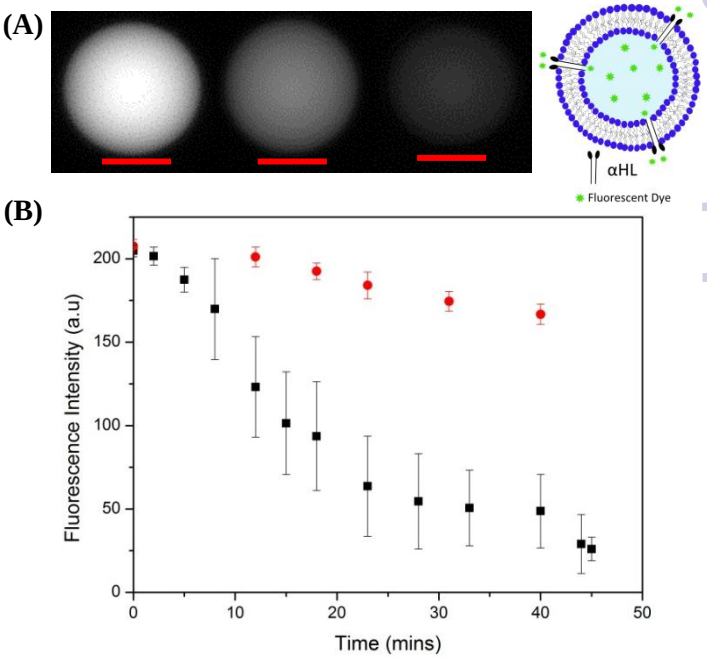

Figure 3: (A) An image series showing the time-dependent (0, 15, 33 minutes respectively) loss of fluorescence in a GUV (scale=30μm). (B) Symmetric vesicles (DPhPC) were loaded with calcein and αHL for multiple GUVs (N=7). Time-dependent loss of calcein fluorescence indicated by black markers and control with calcein fluorescence only (no αHL) indicated by red markers. This signifies that the pore has reconstituted successfully into a functional, unilamellar vesicle membrane.

We performed a series of these experiments using calcein fluorescent dye, both with and without αHL present in the encapsulant (Fig.3).

As can be seen from figure 3, the leakage of calcein was measured following the assembly of αHL into the vesicle bilayer. Over a period of ~40 minutes we observed the gradual decrease of internal fluorescence of the vesicle to reach a point where it was no longer observable. To prove that the decrease was only attributable to the presence of αHL in the membrane, we performed control experiments under the same conditions but without αHL in the encapsulant. The control experiments showed that without the presence of αHL in the vesicles, the fluorescence intensity was maintained over a period of ~40minutes, only a minor decrease was observed due to mild photobleaching of the dye.

Bending rigidity measurements

As mentioned previously one of the main drawbacks of droplet emulsion approaches to form vesicles is the presence of residual solvent in the bilayer. In this study we set out to characterise the GUVs by studying their bending rigidity; the magnitude of this parameter should indicate whether or not presence of oil in the bilayer is found to affect the mechanical properties of the membrane.

To obtain values for bending rigidity of the membrane systems assembled on chip we used fluctuation analysis. This method for measuring membrane bending rigidity was derived by Helfrich[27] and eventually applied to giant vesicles, which have been ubiquitous as a model membrane for studying mechanical properties. GUVs are ideal as a platform for bending rigidity studies as the membrane is fully hydrated and bilayer fluctuations are not constrained by neighbouring membranes or surfaces[28].

Visualisation under the optimal conditions was crucial to observing the thermal fluctuations. As vesicles were constructed of only lipid and aqueous solutions of sucrose and glucose, phase contrast imaging was integral in enhancing the vesicle contour, which in most cases would be difficult to elucidate by eye. Each video was recorded in the equatorial plane of the vesicle, so only fluctuations observable in this plane were analysed.

We studied vesicles which had a concentration gradient across the membrane, the internal aqueous environment comprised of a sucrose solution (400mM, milli-q water) and the external aqueous environment a glucose solution (450mM, milli-q water). This tonicity is essential to ensure that the vesicles are osmotically stable, as well as enhancing the optical contrast of the contours to give clearer images to analyse.

The resulting videos were analysed using custom-made software which maps the changes in the fluctuations of the vesicle shape. The contour fluctuation is broken down into equatorial normal modes using a discrete Fourier transform and the amplitudes of the modes are fitted according to Eqn. 1 to extract bending rigidity.

$$\langle h(q_x, y=0)^2 \rangle = \frac{1}{4L} \frac{k_B T}{\kappa q_x^3}$$

Where h, is the amplitude of the mode q_x, L is the vesicle circumference, K_B is the Boltzmann constant, T is the temperature, σ is the membrane tension, and κ is the bending rigidity.

The equation was manipulated in order for us to fit the data linearly as shown in Eqn. 2.

$$\log \langle h(q_x, y=0)^2 \rangle = -3 \log q_x - \log \frac{K_B T}{4L\kappa} \qquad (2)$$

Therefore, by plotting a graph of log $h(q_x, y = 0)^2$ vs log q_x we were able to fit the data to a straight line with a gradient of -3 (**ESI- SI 2**), with a y-intercept, c corresponding to Eqn. 3.

$$C = \log \frac{K_B T}{4L\kappa} \qquad (3)$$

From this we could obtain a value for the bending rigidity, κ for GUVs generated on chip. Vesicles composed of DPhPC lipid were analysed and a value for bending rigidity was extrapolated. A comparison was drawn between the methods of vesicle generation, the value of symmetric DPhPC vesicles produced *via* our technique is compared with DPhPC vesicles formed *via* electroformation reported previously[29].

A value of 1.29±0.37 $x10^{-19}$J was obtained for symmetric DPhPC populations of GUVs (*N=15*) respectively. This value correlates strongly with the reported literature value of 1.17±0.10 $x10^{19}$J and is within the margin of error[29]. This confirms the integrity of our technique with respect to using microfluidic GUVs as a platform for mechanical property studies. These findings also confirm that the presence of any residual oil in the bilayer has no significant impact on the rigidity of the membrane in microfluidic vesicles.

Conclusion

We have developed a robust microfluidic technique for generating monodisperse GUVs in high-throughput and characterised these systems by studying their mechanical properties using fluctuation analysis. We have confirmed the presence of a unilamellar membrane bilayer by successfully reconstituting the protein pore, αHL, and observing the leakage of fluorescence from the membrane. In order to validate our technique as a legitimate method for producing vesicles, we performed fluctuation analysis to obtain a value for the bending rigidity of compositionally symmetric GUVs. The values we obtained for the GUVs were agreeable with what is reported in literature, which suggests that the quality of vesicles produced *via* our technique is in line with other bulk methods such as electroformation. We have shown that vesicles generated *via* our microfluidic technique are not only monodisperse in size,

compositionally-controlled and generated in rapid throughput, but also act biomimetically with regards to their mechanical properties and membrane rigidity.

Materials and Methods

Phospholipids, 1,2-diphytanoyl-*sn*-glycero-3-phosphocholine (DPhPC), 1-palmitoyl-2-oleoyl-*sn*-glycero-3-phosphocholine (POPC) and 1,2-dioleoyl-*sn*-glycero-3-phosphoethanolamine-N-(lissamine rhodamine B sulfonyl) were obtained from Avanti Polar Lipids (Alabaster, USA). Squalene (Acros Organics, Antwerp) was used as the oil carrier phase. α-hemolysin from *Staphylococcus aureus* (lyophilized powder) was obtained from Sigma-Aldrich (Dorset, UK). Poly(dimethylsiloxane) (PDMS) prepolymer and curing agent kits (Sylgard 184) were obtained from Dow Corning (Midland, MI, USA). Silicon wafers were obtained from IBD Technologies Ltd (Wiltshire, UK). SU-8 negative photoresists and EC development solvent were obtained from Chestech Ltd (Rugby, UK). Poly(dimethylsoloxane-b-ethylene oxide) (PEO) required for the hydrophilic modification of PDMS was obtained from Polysciences Europe GmbH (Eppelheim, Germany). All other chemicals were purchased from Sigma-Aldrich (Dorset, UK).

Device fabrication

The PDMS microfluidic device was fabricated by means of double-layer photolithography[30]. The 'step' was generated by aligning two microchannels and applying different negative photoresists onto the silicon wafer. After development using microdeposit EC solvent, the negative master was exposed to 1,1,2,2-perfluorooctyltrichlorosilane vapour to suppress permanent adhesion to moulded PDMS.

PDMS prepolymer and curing agent were then thoroughly mixed in a 10:1 ratio, and the mixture was poured onto the master wafer. After curing at 65˚C for 3 hours, PDMS treated with 3% PEO surfactant was mixed; the deeper microchannel [to contain the external aqueous phase] was extricated from the cured PDMS and the PEO-PDMS was applied to this individual channel and cured at 65˚C for a further 3 hours. This was necessary to prevent the wetting of the droplets to the channel surface. The PDMS device was bonded *via* partial curing of PDMS spin-coated across a microscopic glass slide.

Preparation of fluids for vesicle generation

Vesicles were composed of 1,2-diphytanoyl-*sn*-glycero-3-phosphocholine (DPhPC) and 1-palmitoyl-2-oleoyl-*sn*-glycero-3-phosphocholine (POPC). The internal aqueous phase (the encapsulant) was prepared using milli-q water and sucrose (400mM), the solution was sonicated for ~45 minutes to dissolve the sucrose and was then filtered. The lipid/oil mixture was prepared to give a 5mg/ml^{-1} concentration; lipid (DPhPC or POPC) was pre-dissolved in chloroform, which was removed under a stream of nitrogen to give a lipid film. Squalene was added and the mixture sonicated for ~60 minutes to ensure the lipid had dissolved fully.

The external aqueous mixture was prepared with sonicated lipid vesicles. The lipid was dissolved in chloroform to give a lipid film, which was then dried under a nitrogen stream. Milli-q water was added to give a concentration of 3mg/ml^{-1} of lipid. Glucose was added to this aqueous solution to a concentration of 450mM. The solution was vortexed to give a turbid mixture and then sonicated for ~60 minutes to give a clear solution for the external aqueous phase.

Microfluidic generation of GUVs

The chip was set up with the three fluid inlets and one vesicle outlet. The internal aqueous phase and oil phase were injected using 1ml plastic syringes linked to 1.09mm PTFE tubing (Adtech Polymer Engineering Ltd, Stroud, UK). The external aqueous phase was injected using a 6ml plastic syringe linked to the same tubing. Three syringe pumps (Chemyx Inc, Stafford, UK) were necessary to pump the reagents into the microfluidic system at controlled flow rates. Aqueous droplets were generated at the flow-focusing junction (Fig.1A). Oil-lipid carrier phase was driven into the device via the oil-lipid inlet (indicated in Fig.1). The internal aqueous phase was driven into the device at the Aq_{IN} inlet (0.10μl min^{-1}). The droplets were carried through the meander channel to the step junction were they were transferred into a wider, deeper channel containing the external aqueous environment. The oil carrier phase delivered the droplets to the aqueous channel as the droplets underwent a phase transfer across the oil-water interface. The phase transfer of the emulsions into the external aqueous medium was density-driven due to the sucrose/glucose concentration gradient of the solutions.

Fluorescence-labelling of the membrane

The vesicles were prepared as previously described however the fluorescent lipid, 1,2-dioleoyl-*sn*-glycero-3-phosphoethanolamine-N-(lissamine rhodamine B sulfonyl) (Rh-PE), was added to the oil-lipid phase in a 0.5 wt% mol concentration.

Protein insertion experiments

The vesicles were prepared as previously described however the internal aqueous encapsulant was prepared with α-hemolysin protein (100ng/μl^{-1}) and calcein fluorescent dye (0.05mM). The solution was buffered to pH 7.4 using NaOH to ensure the full solvation of the calcein dye. The fluorescent protein solution was delivered to the device via the Aq_{IN} inlet and droplets were formed under the usual flow conditions.

Bending Rigidity Measurements

The vesicles were prepared as previously described with the internal aqueous phase composed of sucrose solution (400mM) and the external aqueous phase a glucose extruded lipid solution (450mM). Vesicles were generated, collected and viewed in homemade PDMS wells. The vesicles were generated and visualised at T=25˚C using phase contrast microscopy at a frame rate of ~120 per second. 60 second recordings of the vesicles fluctuating were taken. The contours of the DPhPC GUV populations were analysed. The contours were analysed in terms of the equatorial normal modes of fluctuation, the fitting regime is described in more depth by Yoon *et al*[19].

Process Visualisation and fluorescence

All microfluidic experiments were imaged with a Leica DM IRB microscope. Fluorescence experiments were visualised with a Nikon

Eclipse TE2000-E inverted microscope. The fluorescent species were illuminated using a mercury arc lamp with the appropriate filter sets. Fluorescent images were taken at 100ms exposure time. Images were taken with a QICAM camera (QImaging) and were analysed using ImageJ software. Vesicle fluctuations were imaged using phase contrast on the Nikon Eclipse.

Acknowledgements

This work was supported by EPSRC *via* grants EP/J017566/1 and by an EPSRC Centre of Doctoral Training Studentship from the Institute of Chemical Biology (Imperial College London) awarded to KK.

Notes and references

1. M. Kreir, C. Farre, M. Beckler, M. George, and N. Fertig, *Lab Chip*, 2008, **8**, 587–95.
2. T. M. Allen and P. R. Cullis, *Adv. Drug Deliv. Rev.*, 2013, **65**, 36–48.
3. H. a Rongen, a Bult, and W. P. van Bennekom, *J. Immunol. Methods*, 1997, **204**, 105–33.
4. G. W. and P. R. C. M. J. Hope, M. B. Bally, *Biochim. Biophys. Acta - Rev. Biomembr.*, 1985, **812**, 55–65.
5. M. I. Angelova and D. S. Dimitrov, *Faraday Discuss. Chem. Soc.*, 1986, **81**, 303–311.
6. M. Hishida, H. Seto, N. L. Yamada, and K. Yoshikawa, *Chem. Phys. Lett.*, 2008, **455**, 297–302.
7. D. J. Paterson, J. Reboud, R. Wilson, M. Tassieri, and J. M. Cooper, *Lab Chip*, 2014, **14**, 1806–10.
8. A. deMello and D. van Swaay, *Lab Chip*, 2013, **13**, 752–767.
9. J. Derganc, B. Antonny, and A. Copič, *Trends Biochem. Sci.*, 2013, **38**, 576–84.
10. A. G. Lee, *J. Biol.*, 2009, **8**, 86.
11. M. L. Kirsten, R. a Baron, M. C. Seabra, and O. Ces, *Mol. Membr. Biol.*, 2013, **30**, 303–14.
12. G. S. Attard, A. N. Hunt, S. Jackowski, M. Baciu, S. C. Sebai, X. Mulet, J. A. Clarke, R. V Law, C. Plisson, C. A. Parker, A. Gee, O. Ces, and R. H. Templer, *Biochem. Soc. Trans.*, 2007, **35**, 498–501.
13. G. Niggemann, M. Kummrow, and W. Helfrich, *J. Phys. II*, 1995, **5**, 413–425.
14. J. Pan, S. Tristram-Nagle, N. Kucerka, and J. F. Nagle, *Biophys. J.*, 2008, **94**, 117–24.
15. R. S. Gracià, N. Bezlyepkina, R. L. Knorr, R. Lipowsky, and R. Dimova, *Soft Matter*, 2010, **6**, 1472.
16. W. Rawicz, K. C. Olbrich, T. McIntosh, D. Needham, and E. Evans, *Biophys. J.*, 2000, **79**, 328–39.
17. J. T. J. and W. W. W. M. B. Schneider, *J. Phys.*, 1984, **45**, 1457–1472.
18. Scott T. Miller and S. A. Safran, *Phys. Rev. A*, 1987, **36**, 4371–4379.
19. Y. Z. Yoon, J. P. Hale, P. G. Petrov, and P. Cicuta, *J. Phys. Condens. Matter*, 2010, **22**, 062101.
20. M. Yao and J. Fang, *J. Micromechanics Microengineering*, 2012, **22**, 025012.
21. D. Saeki, S. Sugiura, T. Kanamori, S. Sato, and S. Ichikawa, *Lab Chip*, 2010, **10**, 357–62.
22. P. C. Hu, S. Li, and N. Malmstadt, *ACS Appl. Mater. Interfaces*, 2011, **3**, 1434–40.
23. D. L. Richmond, E. M. Schmid, S. Martens, J. C. Stachowiak, N. Liska, and D. a Fletcher, *Proc. Natl. Acad. Sci. U. S. A.*, 2011, **108**, 9431–6.
24. S. Matosevic and B. M. Paegel, *J. Am. Chem. Soc.*, 2011, **133**, 2798–800.
25. S. Ota, S. Yoshizawa, and S. Takeuchi, *Angew. Chem. Int. Ed. Engl.*, 2009, **48**, 6533–7.
26. E. Gouaux, M. Hobaugh, and L. Song, *Protein Sci.*, 1997, 2631–2635.
27. W. Helfrich, *Zeitschrift fur Naturforsch. Tl. C Biochem. Biophys. Biol. Virol.*, 1973, **28**, 693–703.
28. R. Dimova, *Adv. Colloid Interface Sci.*, 2014, **208**, 225–34.
29. V. Vitkova, P. Méléard, T. Pott, and I. Bivas, *Eur. Biophys. J.*, 2006, **35**, 281–6.
30. P. J. Hung, P. J. Lee, P. Sabounchi, N. Aghdam, R. Lin, and L. P. Lee, *Lab Chip*, 2005, **5**, 44–8.

